Theoretical Study of 1,3-Dipolar Cycloaddition Reactions with Inverse Electron Demand − A DFT Study of the Lewis Acid Catalyst and Solvent Effects in the Reaction of Nitrones with Vinyl Ethers

Luis R. Domingo[a]

Keywords: Inverse electron demand / 1,3-Dipolar cycloadditions / Lewis acids / Solvent effects / Mechanisms / Density functional calculations

The molecular mechanism for the inverse electron demand 1,3-dipolar cycloaddition of nitrones with vinyl ethers has been characterized using density functional theory methods with the B3LYP functional and the 6–31G* basis set. Relative rates, regioselectivity, *endo/exo* stereoselectivity, Lewis acid catalyst and solvent effects are analyzed and discussed. Four reactive channels associated with the formation of two pairs of diasteromeric regioisomers have been characterized. Analysis of the geometries of the corresponding transition structures shows that the reaction in the gas phase takes place by an asynchronous concerted mechanism. These 1,3-dipolar cycloadditions present a large *ortho* regioselectivity, while the *exo* stereoselectivity depends on steric hindrance that appears along the *endo* approach. The inclusion of Lewis acids and solvent effects increase the asynchronicity and contribute a rate acceleration due to a decrease of the activation enthalpies associated with the most favorable *ortho* reactive channels. Both increase the electrophilic character of the nitrone, changing the mechanism; these cycloadditions take place by means of a nucleophilic attack of the vinyl ether on the Lewis acid coordinated nitrone, with concomitant ring closure, and without participation of an intermediate.

Introduction

The cycloaddition of 1,3-dipolar species to an alkene for the synthesis of five-membered rings is a classic reaction in organic chemistry. These 1,3-dipolar cycloaddition (1,3-DC) reactions are used for the preparation of molecules of fundamental importance for both academia and industry.[1] The development of 1,3-DC reactions has in recent years entered a new stage; control of the stereochemistry (regio-, diastereo-, and enantioselectivity) in the addition step now constitutes the major challenge. The stereochemistry of these reactions can be controlled either by choosing the appropriate substrates or by controlling the reaction with a metal complex acting as catalyst.[1] The 1,3-DC reaction between the nitrone **1** and the alkene **2** gives the isoxazolidine **3** (see Scheme 1), which is important, for example, for the preparation of natural products such as β-amino alcohols and alkaloids.[1,2]

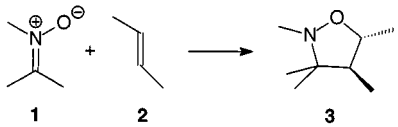

Scheme 1

The typical 1,3-DC reaction of nitrones with substituted alkenes involves a dominant $HOMO_{nitrone}-LUMO_{alkene}$ interaction, which is enhanced by the presence of electron-withdrawing substituents on the dipolarophile.[1,3] The inverse electron demand (IED) 1,3-DC reaction of nitrones with electron-rich alkenes requires a dominant $HOMO_{alkene}-LUMO_{nitrone}$ interaction, since the presence of the electron-releasing substituent on the dipolarophile raises the energies of the frontier molecular orbitals (FMOs). Consequently, such reactions require the activation of the nitrone, and only a few examples are known in which the nitrone is activated by a Lewis acid prior to the reaction with an electron-rich alkene.[4]

Recently, Jorgensen et al.[5] have reported the IED 1,3-DC reaction of the nitrone **4** with the vinyl ether **5** to give exclusively the 5-substituted isoxazolidine **6** (see Scheme 2). The rate of the cycloaddition is enhanced by the presence of a Lewis acid. The reaction is characterized by total *ortho* regioselectivity, while the *exo* stereoselectivity depends on the bulky chiral Lewis acid used as a catalyst.

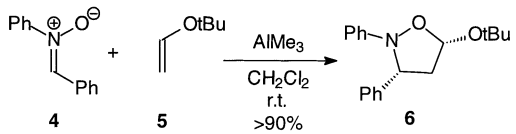

Scheme 2

Several theoretical treatments have been devoted to the study of 1,3-DC reactions of nitrones with substituted alkenes.[6−8] However, this type of cycloaddition has not received the same amount of attention as its counterpart, the Diels−Alder reaction.[9]

[a] Departamento de Química Orgánica, Universidad de Valencia, Dr. Moliner 50, 46100 Burjassot, Valencia, Spain
E-mail: domingo@utopia.uv.es

Supporting information for this article is available on the WWW under http://www.wiley-vch.de/home/eurjoc or from the author.

  1434−193X/00/0612−2265 $ 17.50+.50/0

Recently, Houk et al. have studied the 1,3-DC reaction of the simplest nitrone with methyl vinyl ether, finding in the gas phase an *endo* selectivity along a concerted cycloaddition process.[7] The regioselectivity of these cycloadditions has recently been studied by Magnusong and Pranata.[8] For the reaction between the simplest nitrone and vinylamine the *ortho* regioisomers are preferred over the *meta* ones. However, neither investigation was devoted to the study of the effect of the Lewis acid catalyst on IED 1,3-DC reactions.

Our research program has long maintained an interest in the study of the molecular mechanism of cycloaddition reactions in order to predict their regio- and stereochemical outcome and to shed light on the mechanistic details of these important processes. In the present work, a density functional theory (DFT) study for the IED 1,3-DC reaction between the nitrone **R1** and methyl vinyl ether **R2** including Lewis acid catalyst and solvent effects, as a model of Jorgensen′s reaction, has been carried out in order to understand mechanistic details for this sort of Lewis acid-catalyzed cycloaddition (see Scheme 3).

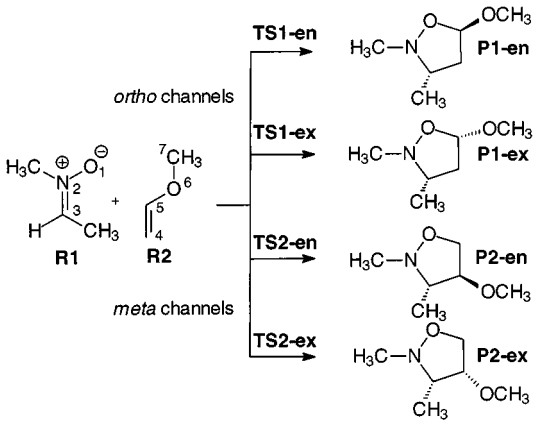

Scheme 3

Computing Methods and Computational Models

In recent years, theoretical methods based on the DFT[10] have emerged as an alternative to traditional ab initio methods in the study of structure and reactivity of chemical systems. Diels−Alder reactions and related cycloaddition reactions have been the object of several density functional studies, showing that functionals that include gradient corrections and hybrid functionals, such as B3LYP, together with the 6−31G* basis set, lead to potential energy barriers in good agreement with the experimental results.[11−13] Thus, in the present study, geometrical optimizations of the stationary points along the potential energy surface (PES) were carried out using the gradient-corrected function of Becke and of Lee, Yang and Parr (B3LYP)[14] for exchange and correlation, with the standard 6−31G* basis set.[15] The stationary points were characterized by frequency calculations in order to verify that minima and transition structures (TSs) have zero and one imaginary frequency, respectively. The optimizations were carried out using the Berny analytical gradient optimization method.[16] The transition vectors (TV,[17] i.e., the eigenvector associated with the unique negative eigenvalue of the force constants matrix) have been characterized. All calculations were carried out with the Gaussian 98 suite of programs.[18] Optimized geometries of all structures are available from the author. The electronic structures of stationary points were analyzed by the natural bond orbital (NBO) method.[19]

Since the different reactive channels present asynchronous TSs, biradical structures could in principle be involved. This has been ruled out by obtaining the wave functions of all TSs with unrestricted DFT theory, and using the keyword STABLE in Gaussian 98. UB3LYP/6−31G* calculation predicts the same TSs as the restricted B3LYP/6−31G*, ruling out the presence of more stable biradical species.[12] Moreover, the HOMO−LUMO energy gap (ca. 4.6 eV), together with the large singlet-triplet splitting energy at TSs (ca. 50 kcal mol^{-1}), forbid the presence of biradical structures.

Energy values (enthalpies, entropies and free energies) have been estimated by means of the potential energy barriers computed at the B3LYP/6−31G* level along with the B3LYP/6−31G* harmonic frequencies. These frequencies have been scaled by 0.96.[20] The energies have been computed at 25 °C, which was the experimental temperature.[5] The enthalpy and entropy changes have been calculated from standard statistical thermodynamic formulas.[15,21]

It is well known that the use of Lewis acids can lead to significant changes in the nature of the molecular mechanism in comparison with the uncatalyzed process. The effect of catalysts in cycloaddition reactions has also been the object of several theoretical studies.[12,22,23] These works predict that the catalyst produces a notable increase in the asynchronicity of the TSs. The effects of the Lewis acid catalyst have been considered using BH_3 as a computational model. This system has been used by different authors to model the presence of Lewis acids with good results.[12,23]

Solvent effects have been considered by B3LYP/6−31G* optimizations of stationary points using a relatively simple self-consistent reaction field (SCRF) method,[24] based on the polarizable continuum model (PCM) of Tomasi's group.[25] In this procedure the solvent is assimilated as a continuous medium, characterized by the dielectric constant (ε), which surrounds a molecule-shaped cavity in which the solute is placed. As the solvent used in the experimental work is dichloromethane, we have used its dielectric constant ε = 8.93.[26] This methodology has been successfully used for the study of related cycloaddition reactions.

As computational models, we have used the simplified dimethyl nitrone **R1** instead of Jorgensen's benzylidenephenylamine *N*-oxide (**4**), and the bulky *tert*-butyl group of the vinyl ether **5** has been replaced by a methyl group. The $AlMe_3$ used as the Lewis acid was modeled by BH_3. Finally, these computational models have been tested optimizing the most favorable *ortho* reactive channels with Jorgensen′s models.

Results and Discussions

I. 1,3-DC Reaction of the Nitrone R1 with Methyl Vinyl Ether (R2) in the Gas Phase

i) Energies

The 1,3-DC reaction of the nitrone **R1** with methyl vinyl ether (**R2**) can take place along four reactive channels corresponding to the *endo* and *exo* approaches of the dipolarophile **R2** to the dipole **R1** in two possible regioisomeric senses: the *ortho* (head-to-head) and *meta* (head-to-tail) pathways (see Scheme 3). The stereoisomeric channels along the *ortho* pathways correspond to the O1−C5 and C3−C4 bond-forming processes, whereas the *meta* pathways correspond to the O1−C4 and C3−C5 ones. Thus, we have studied four TSs: **TS1-en**, **TS1-ex**, **TS2-en** and **TS2-ex**; and four cycloadducts: **P1-en**, **P1-ex**, **P2-en** and **P2-ex**, corresponding to the *endo* and *exo* approaches of the dipolarophile to the dipole, along the *ortho* and *meta* pathways respectively.

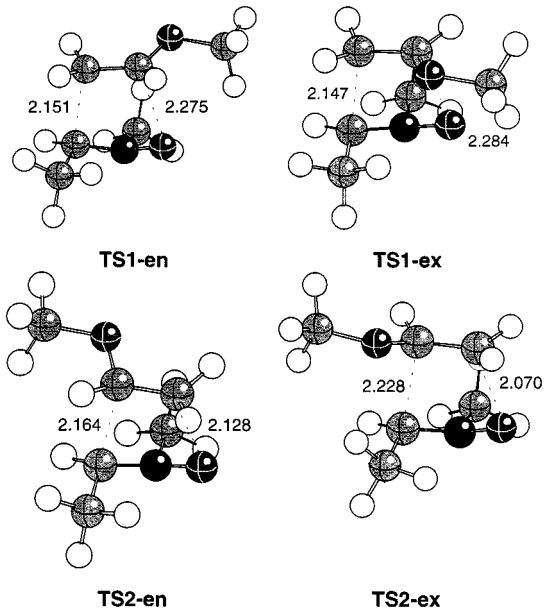

Figure 1. Transition structures for the 1,3-DC reaction between the nitrone **R1** and methyl vinyl ether (**R2**); the values of the bond lengths directly involved in the processes are given in Å

Table 1. Relative energies [enthalpies (ΔH, kcal mol^{-1}), entropies (ΔS, cal mol^{-1} K^{-1}) and free energies (ΔG, kcal mol^{-1}) at 25 °C] for TSs and cycloadducts of the 1,3-DC reaction between the nitrone **R1** and the vinyl ether **R2**

	ΔH	ΔS	ΔG
TS1-en	14.7	−44.3	27.7
TS1-ex	14.1	−43.6	26.9
TS2-en	21.0	−43.5	33.8
TS2-ex	23.5	−44.0	36.4
P1-en	−27.4	−47.6	−13.4
P1-ex	−27.1	−51.5	−12.0
P2-en	−18.0	−47.3	−4.2
P2-ex	−16.0	−46.7	−2.3

A schematic representation of the stationary points along the four reactive channels is presented, together with the atom numbering, in Scheme 3, while Figure 1 presents the geometries of the TSs corresponding to the 1,3-DC reaction. Table 1 reports the values of the relative enthalpies, entropies and free energies for the different stationary points along the four reactive channels.

From these TSs the related minima associated with the final cycloadducts can be obtained. The *ortho* cycloadducts, **P1-en** and **P1-ex**, and the *meta* ones, **P2-en** and **P2-ex**, are two pairs of diastereomers with similar energies. All cycloaddition pathways are highly exothermic processes (the reaction enthalpies are between −27.4 and −16.0 kcal mol^{-1} respectively), the *ortho* cycloadducts being ca. 9 kcal mol^{-1} more stable than the *meta* ones. The greater stability of the *ortho* relative to the *meta* cycloadducts is due to an anomeric effect that occurs between the O1 oxygen atom of the nitronate and the O6 oxygen atom of the methyl ether, which stabilizes the axial arrangement of the methyl ether present in the *ortho* cycloadducts.[27]

The analysis of the activation enthalpies for the TSs reveals that the *ortho* approaches are favored over the *meta* ones; the **TS1-en** and **TS1-ex** are less energetic than **TS2-en** and **TS2-ex**, in the range of 6.9−9.4 kcal mol^{-1}. Therefore, there is a pronounced regioselectivity for this 1,3-DC reaction, in agreement with the experimental results. The stereoselectivity measured as the difference of activation enthalpy between the *endo* and *exo* TSs for the more favorable *ortho* attack indicates that this reaction prefers the *exo* selectivity; **TS1-en** is 0.6 kcal mol^{-1} more energetic than **TS1-ex**. The steric hindrance between the methyl ether and the methyl group present at N2 destabilizes the *endo*/*ortho* approach relative to the *exo*/*ortho* one. Thus, this 1,3-DC reaction shows an *exo* stereoselectivity, which depends on the bulk of the substituents present on both dipole and dipolarophile. Single point calculations at B3LYP/6−31++G** level for the four TSs allow us to confirm these selectivities; the *exo* stereoselectivity increases slightly, by ca. 1 kcal mol^{-1}, while the *ortho* regioselectivity presents a similar value.

Houk et al. found an *endo* stereoselectivity for the 1,3-DC reaction of methyl vinyl ether with the simplest nitrone.[7] In the absence of steric hindrance, a favorable hyperconjugative anomeric-type interaction that appears between the two oxygen atoms of the nitrone and the vinyl ether stabilizes the *endo*/*ortho* TS by 0.8 kcal mol^{-1} relative to the *exo*/*ortho* one.[7] This low relative energy agrees with the fact that the *endo*/*exo* stereoselectivity for these 1,3-DC reactions depends on the bulk of the substituents present on both nitrone and substituted alkene.

The activation entropies for these cycloadditions are strongly negative (in the range −43.5 to −44.3 cal mol^{-1} K^{-1}), and they are responsible for the increase in the free energy of activation for the most favorable reactive channel to 26.9 kcal mol^{-1}. A similar result is found for the 1,3-DC reactions of the azomethine ylides with acrylonitrile.[13]

ii) Geometrical Parameters and Analysis of Frequencies

The geometries of the TSs corresponding to the four reactive channels are displayed in Figure 1. For the more favorable *ortho* TSs, the lengths of the C3−C4 forming bonds (ca. 2.15 Å) are slightly shorter than the lengths of the O1−C5 ones (ca. 2.28 Å). Similar forming bond lengths are found for the 1,3-DC reaction between methyl vinyl ether and the simplest nitrone.[7] For the *meta* TSs there is an inversion of the asymmetry, the lengths of the O1−C4 forming bond being shorter than for the C3−C5 ones. Considering that C−O single bonds are slightly shorter than C−C ones, these geometrical parameters show that these cycloadditions correspond to concerted processes.

The C4−C5−O6−C7 dihedral angles at these TSs are ca. 180°. These values are similar to those found for the cycloaddition reactions of methyl vinyl ether with a variety of dienes and dipoles, and permits efficient delocalization of the lone pair of the O6 oxygen atom in the dipolarophile system along the *ortho* reactive pathways.[7,12]

The dominant transition vector components for these TSs are associated with the bond lengths corresponding to the two σ bonds that are formed along these 1,3-DC processes. The values of the C3−C4 components for the *ortho* TSs, in the range 0.71−0.79, are larger than for the O1−C5 ones, in the range 0.45−0.48, showing the asynchronicity of these cycloaddition processes.

Several bond angles and dihedral angles also participate in the transition vectors. Thus, the C3−C4−H4a and C3−C4−H4b components are associated with the hybridization change developing at the C4 center on transforming from sp^2 to sp^3, while the different dihedral angles are also associated with the hybridization change that is developing at the N2 center on going from sp^2 to sp^3.

The imaginary frequency values for the *ortho* TSs **TS1-en** and **TS1-ex** (442i and 429i cm^{-1}, respectively) are slightly lower than those for the *meta* TSs **TS2-ex** and **TS2-ex** (489i and 484i cm^{-1}, respectively). These results are similar to those found for related cycloaddition reactions where the more asynchronous TSs have the lower imaginary frequency.[12,13]

iii) Bond Order and Charge Analysis

The extent of bond formation or bond breaking along a reaction pathway is provided by the concept of bond order (BO). This theoretical tool has been used to study the molecular mechanism of chemical reactions.[28] To follow the nature of the these processes, the Wiberg bond indices[29] have been computed by using the NBO analysis as implemented in Gaussian 98. The results are included in Table 2.

The BO analysis shows that these TSs correspond to asynchronous concerted processes, the *ortho* TSs being more asynchronous than the *meta* ones. For the former, the BOs for the O1−C5 forming bonds (0.28) have lower values than for the C3−C4 ones (0.40), indicating a C−C bond formation more advanced than the C−O one. The similar BO values found for the two σ bonds that are being formed at the *meta* TSs indicates a more synchronous bond formation process (see Table 2).

Table 2. Wiberg bond orders at the transition structures **TS1-en**, **TS1-ex**, **TS2-en** and **TS2-ex**

	TS1-en	TS1-ex		TS2-en	TS2-ex
O1−C2	1.18	1.18	O1−C2	1.22	1.20
N2−C3	1.31	1.31	N2−C3	1.28	1.27
C3−C4	0.40	0.40	C3−C5	0.40	0.39
C4−C5	1.50	1.51	C4−C5	1.50	1.48
O1−C5	0.28	0.27	O1−C4	0.36	0.38
C5−O6	1.01	1.02	C5−O6	0.94	0.95

A comparison of the results presented in Table 1 with those in Table 2 shows a relationship between the activation enthalpies of the four TSs and the asynchronicity of the processes. The less energetic *ortho* TSs are more asynchronous than the *meta* ones. This fact supports the empirical role that holds for a variety of [4+2] cycloaddition reactions that "for asymmetrically substituted dienophiles, the more asynchronous TS has the lower energy".[11e,12,13]

Natural population analysis for the TSs gives a small charge transfer from the vinyl ether to the nitrone. The charge transfer at the *ortho* TSs (0.06 and 0.07e, for **TS1-en** and **TS1-ex**, respectively) is slightly larger than at the *meta* ones (0.02 and 0.03e, for **TS2-en** and **TS2-ex**, respectively). This low charge transfer found for these IED 1,3-DC reactions can be related to the electron-rich character of the nitrone, which prevents the charge transfer from the electron-rich alkene during the cycloaddition process.

Finally, the FMO analysis allows us to understand the electronic nature of this 1,3-DC reaction (see Figure 2). The presence of the electron-releasing $-OCH_3$ group on the substituted alkene **R2** raises the HOMO and LUMO energies. This fact is responsible for the $HOMO_{alkene}-LUMO_{nitrone}$ interaction being more favorable than the $HOMO_{nitrone}-LUMO_{alkene}$ ones, and confirms the IED nature of this cycloaddition.

iv) 1,3-DC Reaction of the Nitrone 4 with *tert*-Butyl Vinyl Ether (5)

Finally, the most favorable *ortho* reactive channels corresponding to the 1,3-DC reaction between Jorgensen's benzyl-

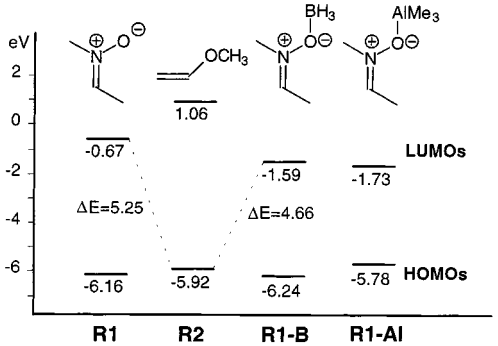

Figure 2. FMO interactions in the 1,3-DC reactions between the nitrone **R1** and methyl vinyl ether **R2**; the FMO of the BH_3-coordinated nitrone **R1−B** and $AlMe_3$-coordinated nitrone **R1-Al** are also included

idenephenylamine *N*-oxide (**4**) and the bulky *tert*-butyl vinyl ether (**5**) have been studied in order to test our computational models. Figure 3 shows the geometries of the corresponding *ortho*/*endo* and *ortho*/*exo* TSs, **TS3-en** and **TS3-ex**, respectively.

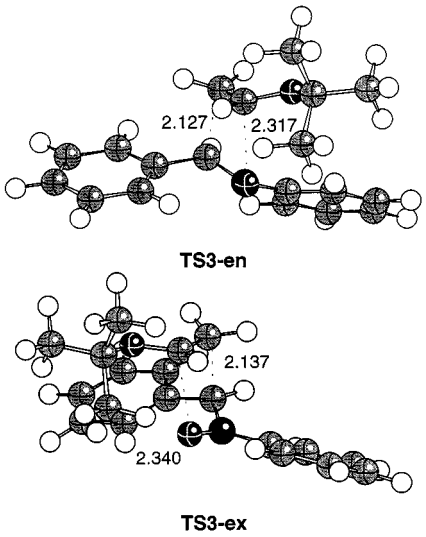

Figure 3. Transition structures corresponding to the *ortho* reactive channels of the 1,3-DC reaction between the nitrone **4** and the vinyl ether **5**; the values of the bond lengths directly involved in the processes are given in Å

Substitution of the two phenyl groups on Jorgensen's nitrone **4** by two methyl groups does not significantly change the results obtained in this study. Both potential energy barriers and *exo* stereoselectivity increase slightly relative to those for the small model **R1** + **R2** (1.6 and 2.3 kcal mol^{-1}, respectively) because of an increase in the unfavorable steric hindrance that appears between the bulky phenyl and *tert*-butyl groups.

A comparison of the lengths of the two forming bonds between **TS1-en** and **TS1-ex**, and **TS3-en** and **TS3-ex** (see Figure 1 and 3) indicates similar bond formation for both cycloaddition processes; Jorgensen's model being slightly more asynchronous than the reduced model, due to a lengthening of the O1−C5 forming bond as a consequence of the unfavorable steric hindrance. These findings allow us to endorse the use of the nitrone **R1** and the vinyl ether **R2** as reduced models for the study of these IED 13-DC reactions; electronic and steric features of Jorgensen's models are both well reproduced.

II) Lewis Acid Catalyst

As stated in the introductory section, the 1,3-DC reactions between nitrones and electron-rich alkenes are promoted in the presence of Lewis acids.[5] Therefore, the effect of a Lewis acid catalyst on the IED 1,3-DC reaction between **R1** and **R2** was studied. All stationary points along the four reactive channels were optimized coordinating the BH_3 Lewis acid to the O1 oxygen atom of the nitrone group in *exo* orientation.[12,22c] The geometries of the corresponding TSs, **TS1-en-B**, **TS1-ex-B**, **TS2-en-B** and **TS2-ex-B**, are depicted in Figure 4, while Table 3 presents the relative energies.

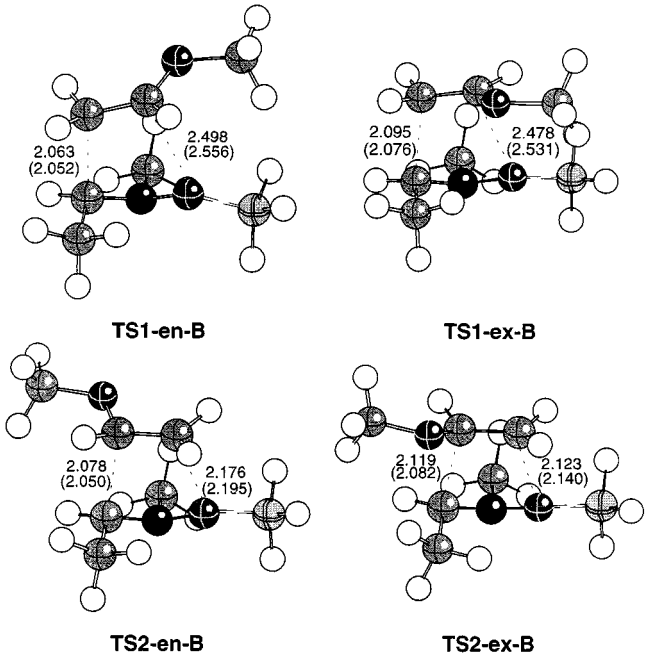

Figure 4. Transition structures for the Lewis acid-catalyzed 1,3-DC reaction between the BH_3-coordinated nitrone **R1−B** and the vinyl ether **R2**; the values of the bond lengths directly involved in the processes are given in Å; the values in parentheses correspond to the reaction in dichloromethane

Table 3. Relative energies [enthalpies (ΔH, kcal mol^{-1}), entropies (ΔS, cal mol^{-1} K^{-1}) and free energies (ΔG, kcal mol^{-1}) at 25 °C] for TSs and cycloadducts of the BH_3-catalyzed 1,3-DC reaction between **R1−B** and **R2**; the activation parameters for the $AlMe_3$-catalyzed 1,3-DC reaction between **R1-Al** and **R2** are also included

	ΔH	ΔS	ΔG
TS1-en-B	11.6	−44.5	24.7
TS1-ex-B	9.6	−44.7	22.7
TS2-en-B	22.5	−45.4	35.8
TS2-ex-B	24.8	−45.3	38.1
P1-en-B	−16.9	−47.9	−2.8
P1-ex-B	−16.0	−48.5	−1.8
P2-en-B	−9.6	−48.7	4.6
P2-ex-B	−7.6	−48.7	6.7
TS1-en-Al	11.8	−41.9	24.1
TS1-ex-Al	10.7	−41.3	22.8

The Lewis acid catalyst has a different influence on the two regioisomeric pathways. The presence of the Lewis acid decreases the activation enthalpies for *ortho* cycloadditions by 3.1 to 4.5 kcal mol^{-1}, compared with those for the uncatalyzed processes, while for the *meta* additions there are increases in the range of 1.3 to 1.5 kcal mol^{-1}. Moreover, the inclusion of the Lewis acid catalyst increases by 1.4 kcal mol^{-1} the *exo* stereoselectivity for the more favorable *ortho* channels. The inclusion of the Lewis acid does not modify significantly the activation entropies. Consequently, the decrease in activation enthalpies is responsible for the decrease of free energies of activation for the catalyzed process.

The influence of Lewis acid catalysts has been found in previous studies on related Diels−Alder reactions,[12] and it can be understood in terms of a stronger interaction between the $HOMO_{dipolarophile}-LUMO_{dipole}$. Figure 2 shows the decrease of the $LUMO_{dipole}$ energy for the BH_3-coordinated nitrone, **R1-B**, relative to that for **R1** (ΔE = 0.92 eV); this effect decreases the $HOMO_{dipolarophile}-LUMO_{dipole}$ energy gap, in agreement with the lowering of the activation enthalpy found for the catalyzed process.

There is a more noticeable change in the structural features of the BH_3-coordinated TSs. The Lewis acid catalyst enhances significantly the asynchronicity of bond formation process for the more favorable *ortho* TSs, along an increase of the O1−C5 distance (see Figure 3). This behavior is also observed in the BO analysis. The C3−C4 BO values for **TS1-en-B** and **TS1-ex-B** are 0.45 and 0.42, respectively, while the O1−C5 ones are 0.16, indicating that these processes are highly asynchronous (see Table 4).

Table 4. Wiberg bond orders in the transition structures **TS1-en-B**, **TS1-ex-B**, **TS2-en-B** and **TS2-ex-B**

	TS1-en-B	TS1-ex-B		TS2-en-B	TS2-ex-B
O1−C2	1.05	1.05	O1−C2	1.09	1.08
N2−C3	1.32	1.32	N2−C3	1.28	1.27
C3−C4	0.45	0.42	C3−C5	0.44	0.43
C4−C5	1.47	1.49	C4−C5	1.47	1.45
O1−C5	0.16	0.15	O1−C4	0.30	0.32
C5−O6	1.11	1.10	C5−O6	0.92	0.96

The C5−O6 BO values at the *ortho* TSs are slightly larger than those for the *meta* ones. These data account for a favorable delocalization of the lone pair of the O6 oxygen atom in the *ortho* TSs, which increases the nucleophilic character of the vinyl ether.[12] The Lewis acid catalyst does not modify the asynchronicity significantly for the less favorable *meta* TSs.

Natural population analysis for the catalyzed TSs shows an large increase in charge transfer from the electron-rich vinyl ether to the BH_3-coordinated nitrone. This is larger for the *ortho* TSs (0.24 e) than for the *meta* ones (0.16 e).

However, the most noticeable effect of the Lewis acid is the large delocalization of negative charge on the BH_3 fragment at **R1−B** and TSs (ca. 0.3 e), which increases the electrophilic character of the nitrone, favoring the charge transfer process.[12] This fact allows us to explain the large charge transfer found in the catalyzed processes (ca. 0.2 e) relative to the uncatalyzed ones.

The role of the Lewis acid catalyst in these IED 1,3-DC reactions can be interpreted as an increase in the electrophilic character of the nitrone, which allows a stabilization of the corresponding TS by delocalization of the negative charge that is being transferred along the asynchronous cycloaddition process. As a consequence, the Lewis acid has a different effect on the values of the activation enthalpies of the two regioisomeric possibilities. For the *ortho* TSs the charge transfer is favored by the presence of the O6 oxygen atom on the dipolarophile, which stabilizes the incipient positive charge that is developing at the C5 carbon atom of the substituted alkene during the cycloaddition process. For the *meta* TSs this stabilization is not effective, increasing the activation enthalpies.

Finally, the most favorable *ortho* reactive channels of this IED 1,3-DC reaction have been studied using $AlMe_3$ as a Lewis acid catalyst, in order to test the BH_3 computational model. Figure 5 shows the geometries of TSs **TS1-en-Al** and **TS1-ex-Al**, while the relative energies are given in Table 3.

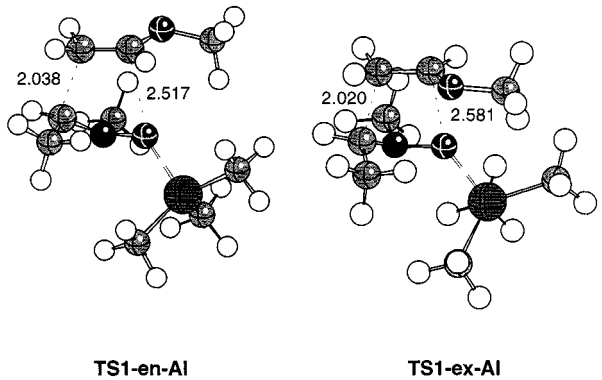

Figure 5. Transition structures corresponding to the *ortho* reactive channels of the Lewis acid-catalyzed 1,3-DC reaction between the $AlMe_3$-coordinated nitrone **R1-Al** and the vinyl ether **R2**; the values of the bond lengths directly involved in the processes are given in Å

Substitution of BH_3 by $AlMe_3$ does not change significantly the results obtained in this study. Thus, while for the most favorable **TS1-ex-Al** the activation enthalpy increases slightly (1.1 kcal mol^{-1}) the *exo* selectivity decreases 0.9 kcal mol^{-1} relative to the BH_3-catalyzed process, due to slightly greater stabilization of **TS1-en-Al**. A comparison of the lengths of the two forming bonds along the two catalyzed cycloadditions (Figure 4 and 5) indicates similar bond formation for both cycloaddition processes. **TS1-en-Al** and **TS1-ex-Al** are slightly more asynchronous than **TS1-en-B** and **TS1-ex-B**. This increase in asynchronicity can be explained by a slight increase in the electrophilic character of **R1-Al** relative to **R1−B,** showed by the lowering of the LUMO energy for **R1-Al** relative to **R1−B** (see Figure 2). Thus, natural population analysis gives a slightly larger transfer for **TS1-en-Al** (0.26 e) than for **TS1-en-B** (0.24 e). This comparative study allows us to endorse the use of the smaller BH_3 Lewis acid as a computational model in the study of the electronic behavior of the Lewis acid catalysts in this type of cycloaddition reactions.

III) Solvent Effects on the Catalyzed 1,3-DC Reaction

Solvent effects on cycloaddition reactions are well-known and have received considerable attention, especially in the last few years. The solvent effects have been examined by B3LYP/6−31G* optimizations of stationary points using a relatively simple SCRF method, based on the PCM of Tomasi's group.[25]

Table 5. Relative enthalpies [ΔH (kcal mol^{-1}) at 25 °C] for TSs and cycloadducts of the BH_3-catalyzed 1,3-DC reaction between **R1-S** and **R2-S** in dichloromethane

TS1-en-S	13.3	**P1-en-S**	−13.4
TS1-ex-S	11.6	**P1-ex-S**	−12.5
TS2-en-S	24.5	**P2-en-S**	−6.7
TS2-en-S	26.4	**P2-ex-S**	−4.9

Table 5 reports the relative enthalpies obtained with the inclusion of solvent effects. Reactants, TSs and cycloadducts are stabilized in the range of 5−8 kcal mol^{-1} relative to gas phase calculations. The most noticeable change with the inclusion of solvent effects is the increase in activation enthalpies (between 1.7 and 2.0 kcal mol^{-1}) and the decrease in exothermicity of the process (between 2.5 and 3.5 kcal mol^{-1}) because of a greater stabilization of the reactants than of TSs and cycloadducts. Moreover, solvent effects decrease the *exo* stereoselectivity slightly (0.3 kcal mol^{-1}) due to greater stabilization of the *endo* TS than the *exo* one.[12,30]

Finally, a comparison of the geometrical parameters given in Figure 4 shows that the inclusion of solvent effects in the geometry optimization increases the asynchronicity for the *ortho* TSs slightly, while for the *meta* TSs there is a decrease. This behavior is also observed in the BO analysis. The C3−C4 BO values for **TS1-en-S** and **TS1-ex-S** are 0.44 and 0.42, respectively, while the O1−C5 ones are 0.13. This low O1−C5 BO value must be attributed to stabilizing factors in **TS1-en-S** and **TS1-ex-S** rather than an O1−C5 bond formation process.[12,31] Moreover, solvent effects also slightly increase the charge transfer for the *ortho* TSs relative to gas phase calculations.

Thus, this catalyzed cycloaddition, which takes place by means of a one-step mechanism, must be considered as a nucleophilic attack of the β-carbon atom of the electron-rich alkene onto the carbon atom of the Lewis acid coordinated nitrone, with concomitant ring closure, rather than as pericyclic process. Consequently, inclusion of Lewis acid catalyst and solvent effects causes a drastic change in the nature of the cycloaddition relative to the noncatalyzed reaction in the gas phase; the Lewis acid catalyzed cycloaddition is now a nonpericyclic reaction.

Conclusions

The molecular mechanism for the IED 1,3-DC reactions of nitrones with vinyl ethers has been studied using density functional theory methods with the B3LYP functional and the 6−31G* basis set. The potential energy surface has been explored and four reactive pathways have been characterized by means of the localization of the corresponding stationary points. Relative rates, regioselectivity and stereoselectivity have been analyzed and discussed. Finally, the Lewis catalyst and solvent effects in these IED 1,3-DC reactions have been considered.

Analysis of the geometries and BOs at the TSs associated with the different reaction pathways shows that in the gas phase these 1,3-DC reactions take place by means of an asynchronous concerted mechanism. These cycloadditions possess a high degree of regioselectivity, while the *exo* stereoselectivity depends on the steric hindrance that appears along the *endo* approach.

Inclusion of Lewis acid and solvent effects increases the asynchronicity of the bond formation process and the charge transfer for the *ortho* cycloadditions. These effects decrease the activation enthalpies for the more favorable *ortho* reactive channels, increasing the rate and regioselectivity of these 1,3-DC reactions. This behavior can be understood as a consequence of a change of mechanism for the catalyzed IED 1,3-DC reaction. Inclusion of Lewis acid and solvent effects causes the nitrone and vinyl ether to behave as an electrophile and a nucleophile respectively, rather than as a dipole and dipolarophile. Thus, these reactions must be considered as a nucleophilic attack of the β-carbon of the vinyl ether at the carbon atom of the Lewis acid-coordinated nitrone.

As a consequence of the results described in this paper, we recommend the inclusion of models for Lewis acid catalyst and solvent effects at high computational level (B3LYP/6−31G*) for theoretical study of the reactive pathways, in particular TSs, related to the regioselectivity and stereoselectivity of cycloaddition reactions involving polar species.

Acknowledgments

This work was supported by research funds provided by the Ministerio de Educación y Cultura of the Spanish Government by DGICYT (project PB98−1429). All calculations were performed on a Cray-Silicon Graphics Origin 2000 of the Servicio de Informática de la Universidad de Valencia. I am most indebted to this center for providing the computer capabilities.

[1] K. V. Gothelf, K. A. Jorgensen, *Chem. Rev.* **1998**, *98*, 863−909.
[2] [2a] J. J. Tufariello, *1,3-Dipolar Cycloaddition Chemistry*; A. Padwa, J. Wiley & Sons, New York, **1984**. − [2b] K. B. G. Torssell, *Nitrile Oxides, Nitrones and Nitronates in Organic Syntesis*, VCH, New York, **1988**. − [2c] J. J. Tufariello, *Acc. Chem. Res.* **1979**, *12*, 396−403.
[3] I. Fleming, *Frontier Orbitals and Organic Chemical Reactions*, J. Wiley & Sons, New York, **1976**.
[4] [4a] J.-P. G. Seerden, A. W. A. Scholte op Reimer, H. W. Scheeren, *Tetrahedron Lett.* **1994**, *35*, 4419−4422. − [4b] J.-P. G. Seerden, M. M. M. Kuypers, H. W. Scheeren, *Tetrahedron: Asymmetry* **1995**, *6*, 1441−1450. − [4c] J.-P. G. Seerden, M. M. M. Boeren, H. W. Scheeren, *Tetrahedron* **1997**, *53*, 11843−11852.
[5] K. B. Simonsen, P. Bayón, R. G. Hazell, K. V. Gothelf, K. A. Jorgensen, *J. Am. Chem. Soc.* **1999**, *121*, 3845−3853.
[6] [6a] K. Tanaka, T. Imase, S. Iwata, *Bull. Chem. Soc. Jpn.* **1996**, *69*, 2243−2248. − [6b] I. Morao, B. Lecea, F. P. Cossío, *J. Org. Chem.* **1997**, *62*, 7033−7036. − [6c] F. P. Cossío, I. Morao, H. Jiao, P. von R. Schleyer, *J. Am. Chem. Soc*. **1999**, *121*, 6737−6746.
[7] J. Liu, S. Niwayama, Y. You, K. N. Houk, *J. Org. Chem.* **1998**, *63*, 1064−1073.
[8] E. C. Magnusong, J. Pranata, *J. Comput. Chem.* **1998**, *19*, 1795−1804.
[9] [9a] J. Sauer, R. Sustmann, *Angew. Chem. Int. Ed. Engl.* **1980**, *19*, 778−807. − [9b] K. N. Houk, J. González, Y. Li, *Acc. Chem. Res.* **1995**, *28*, 81−90.
[10] [10a] R. G. Parr, W. Yang, *Density Functional Theory of Atoms and Molecules*, Oxford University Press, New York, **1989**. − [10b] T. Ziegler, *Chem. Rev.* **1991**, *91*, 651−667.

[11] [11a] E. Goldstein, B. Beno, K. N. Houk, *J. Am. Chem. Soc.* **1996**, *118*, 6036−6043. − [11b] V. Branchadell, *Int. J. Quantum Chem.* **1997**, *61*, 381−388. − [11c] A. Sbai, V. Branchadell, R. M. Ortuño, A. Oliva, *J. Org. Chem.* **1997**, *62*, 3049−3054. − [11d] V. Branchadell, J. Font, A. G. Moglioni, C. Ochoa de Echaguen, A. Oliva, R. M. Ortuno, J. Veciana, J. Vidal Gancedo, *J. Am. Chem. Soc.* **1997**, *119*, 9992−10003. − [11e] J. I. García, V. Martínez-Merino, J. A. Mayoral, L. Salvatella, *J. Am. Chem. Soc.* **1998**, *120*, 2415−2420. − [11f] L. F. Tietze, T. Pfeiffer, A. Schuffenhauer, *Eur. J. Org. Chem.* **1998**, 2733−2741. − [11g] L. R. Domingo, M. Arnó, J. Andrés, *J. Am. Chem. Soc.* **1998**, *120*, 1617−1618.

[12] [12a] L. R. Domingo, M. Arnó, J. Andrés, *J. Org. Chem.* **1999**, *64*, 5867−5875. − [12b] L. R. Domingo, A. Asensio, *J. Org. Chem.* **2000**, *65*, 1076−1083.

[13] L. R. Domingo, *J. Org. Chem.* **1999**, *64*, 3922−3929.

[14] [14a] A. D. Becke, *J. Chem. Phys.* **1993**, *98*, 5648−5652. − [14b] C. Lee, W. Yang, R. G. Parr, *Phys. Rev. B* **1988**, *37*, 785−789.

[15] W. J. Hehre, L. Radom, P. v. R. Schleyer, J. A. Pople, *Ab initio Molecular Orbital Theory*, J. Wiley & Sons, New York, **1986**.

[16] H. B. Schlegel, "Geometry Optimization on Potential Energy Surface", in *Modern Electronic Structure Theory.* (Ed.: D. R. Yarkony), World Scientific Publishing, Singapore, **1994**.

[17] J. W. J. McIver, A. Komornicki, *J. Am. Chem. Soc.* **1972**, *94*, 2625−2633.

[18] M. J. Frisch, G. W. Trucks, H. B. Schlegel, G. E. Scuseria, M. A. Robb, J. R. Cheeseman, V. G. Zakrzewski, J. A. Montgomery Jr., R. E. Stratmann, J. Burant, S. Dapprich, J. M. Millam, A. D. Daniels, K. N. Kudin, M. C. Strain, O. Farkas, J. Tomasi, V. Barone, M. Cossi, R. Cammi, B. Mennucci, C. Pomelli, C. Adamo, S. Clifford, J. Ochterski, G. A. Petersson, P. Y. Ayala, Q. Cui, K. Morokuma, D. K. Malick, A. D. Rabuck, K. Raghavachari, J. B. Foresman, J. Cioslowski, J. V. Ortiz, B. B. Stefanov, G. Liu, A. Liashenko, P. Piskorz, I. Komaromi, R. Gomperts, R. L. Martin, D. J. Fox, T. Keith, M. A. Al-Laham, C. Y. Peng, A. Nanayakkara, C. Gonzalez, M. Challacombe, W. P. M. Gill, B. Johnson, W. Chen, M. W. Wong, J. L. Andres, C. Gonzalez, M. Head-Gordon, E. S. Replogle, J. A. Pople, *Gaussian 98, Revision A.6*, Gaussian, Inc., Pittsburgh PA, **1998**.

[19] [19a] E. D. Glendening, A. E. Reed, J. E. Carpenter, F. Weinhold, *NBO version 3.1 in Gaussian 98*, *Revision A.6*. − [19b] A. E. Reed, R. B. Weinstock, F. Weinhold, *J. Chem. Phys.* **1985**, *83*, 735−746. − [19c] A. E. Reed, L. A. Curtiss, F. Weinhold, *Chem. Rev.* **1988**, *88*, 899−926.

[20] A. P. Scott, L. Radom, *J. Phys. Chem.* **1996**, *100*, 16502−16513.

[21] W. L. Jorgensen, D. Lim, J. F. Blake, *J. Am. Chem. Soc.* **1993**, *115*, 2936−2942.

[22] [22a] B. S. Jursic, Z. Zdravkovski, *J. Org. Chem.* **1995**, *59*, 7732−7736. − [22b] S. Yamabe, T. Dai, T. Minato, *J. Am. Chem. Soc.* **1995**, *117*, 10994−10997. − [22c] W.-M. Dai, C. W. Lau, S. H. Chung, D.-Y. Wu, *J. Org. Chem.* **1995**, *60*, 8128−8129. − [22d] J. González, T. Sordo, J. A. Sordo, *THEOCHEM* **1996**, *358*, 23−27.

[23] [23a] D. M. Birney, K. N. Houk, *J. Am. Chem. Soc.* **1990**, *112*, 4127−4133. − [23b] M. A. McCarrick, Y.-D. Wu, K. N. Houk, *J. Org. Chem.* **1993**, *58*, 3330−3343. − [23c] A. Venturini, J. Joglar, S. Fustero, J. Gonzalez, *J. Org. Chem.* **1997**, *62*, 3919−3926.

[24] [24a] J. Tomasi, M. Persico, *Chem. Rev.* **1994**, *94*, 2027−2094. − [24b] B. Y. Simkin, I. Sheikhet, *Quantum Chemical and Statistical Theory of Solutions − A Computational Approach*, Ellis Horwood, London, **1995**.

[25] [25a] M. T. Cances, V. Mennunci, J. Tomasi, *J. Chem. Phys.* **1997**, *107*, 3032−3041. − [25b] M. Cossi, V. Barone, R. Cammi, J. Tomasi, *Chem. Phys. Lett.* **1996**, *255*, 327−335. − [25c] V. Barone, M. Cossi, J. Tomasi, *J. Comp. Chem.* **1998**, *19*, 404−417.

[26] R. L. David, *CRC Handbook of Chemistry and Physics*, 76th ed., CRC Press, Boca Raton, Florida, **1996**.

[27] C. L. Perrin, K. B. Armstrong, M. A. Fabian, *J. Am. Chem. Soc.* **1994**, *116*, 715−722.

[28] [28a] G. Lendvay, *THEOCHEM* **1988**, *167*, 331−338. − [28b] G. Lendvay, *J. Phys. Chem.* **1989**, *93*, 4422−4429. − [28c] G. Lendvay, *J. Phys. Chem.* **1994**, *98*, 6098−6104.

[29] K. B. Wiberg, *Tetrahedron* **1968**, *24*, 1083−1096.

[30] C. Cativiela, J. I. García, J. A. Mayoral, L. Salvatella, *Chem. Soc. Rev.* **1996**, *25*, 209−218.

[31] [31a] L. R. Domingo, M. T. Picher, R. J. Zaragozá, *J. Org. Chem.* **1998**, *63*, 9183−9189. − [31b] L. R. Domingo, M. T. Picher, M. J. Aurell, *J. Phys. Chem. A* **1999**, 103, 11425−11430.

Received September 16, 1999
[O99531]